Redox Biology 13 (2017) 459–469

Contents lists available at ScienceDirect

Redox Biology

journal homepage: www.elsevier.com/locate/redox

Research Paper

Metabolomics analysis reveals that benzo[a]pyrene, a component of $PM_{2.5}$, promotes pulmonary injury by modifying lipid metabolism in a phospholipase A2-dependent manner *in vivo* and *in vitro*

Song-Yang Zhang[a,1], Danqing Shao[a,1], Huiying Liu[a], Juan Feng[a], Baihuan Feng[b], Xiaoming Song[b], Qian Zhao[b], Ming Chu[c], Changtao Jiang[a], Wei Huang[b,*], Xian Wang[a,*]

[a] Department of Physiology and Pathophysiology, School of Basic Medical Sciences, Peking University, Key Laboratory of Molecular Cardiovascular Science, Ministry of Education and Beijing Key Laboratory of Cardiovascular Receptors Research, Beijing 100191, People's Republic of China
[b] Department of Occupational & Environmental Health Sciences, School of Public Health, Peking University, Beijing 100191, People's Republic of China
[c] Department of Immunology, School of Basic Medical Sciences, Peking University, Beijing 100191, People's Republic of China

ARTICLE INFO

Keywords:
$PM_{2.5}$
Benzo[a]pyrene
Pulmonary injury
Phospholipase A2
Alveolar type II cell

ABSTRACT

Particulate matter with an aerodynamic diameter less than 2.5 μM ($PM_{2.5}$) is one of the major environmental pollutants in China. In this study, we carried out a metabolomics profile study on $PM_{2.5}$-induced inflammation. $PM_{2.5}$ from Beijing, China, was collected and given to rats through intra-tracheal instillation *in vivo*. Acute pulmonary injury were observed by pulmonary function assessment and H.E. staining. The lipid metabolic profile was also altered with increased phospholipid and sphingolipid metabolites in broncho-alveolar lavage fluid (BALF) after $PM_{2.5}$ instillation. Organic component analysis revealed that benzo[a]pyrene (BaP) is one of the most abundant and toxic components in the $PM_{2.5}$ collected on the fiber filter. *In vitro*, BaP was used to treat A549 cells, an alveolar type II cell line. BaP (4 μM, 24 h) induced inflammation in the cells. Metabolomics analysis revealed that BaP (4 μM, 6 h) treatment altered the cellular lipid metabolic profile with increased phospholipid metabolites and reduced sphingolipid metabolites and free fatty acids (FFAs). The proportion of ω–3 polyunsaturated fatty acid (PUFA) was also decreased. Mechanically, BaP (4 μM) increased the phospholipase A2 (PLA2) activity at 4 h as well as the mRNA level of *Pla2g2a* at 12 h. The pro-inflammatory effect of BaP was reversed by the cytosolic PLA2 (cPLA2) inhibitor and chelator of intracellular Ca^{2+}. This study revealed that BaP, as a component of $PM_{2.5}$, induces pulmonary injury by activating PLA2 and elevating lysophosphatidylcholine (LPC) in a Ca^{2+}-dependent manner in the alveolar type II cells.

1. Introduction

With rapid industrialization, haze-fog-associated air pollution, characterized by a high level of particulate matter (PM), has become one of the most severe environmental issues in China [1]. The detrimental effect of PM is mainly determined by its size and composition. Due to its small diameter and large surface area, PM with an aerodynamic diameter less than 2.5 μM ($PM_{2.5}$) carries various toxic components and pathogens into the body and causes harm [2]. Many studies have indicated that there is a close association between mortality and $PM_{2.5}$ level, especially respiratory and cardiovascular mortality [3–6]. As the site for gas exchange and a barrier from the external environment, the respiratory system is exposed directly to high levels of $PM_{2.5}$. $PM_{2.5}$ has been proven to increase the incidence of respiratory diseases, including pneumonia, asthma, chronic obstructive pulmonary disease (COPD) and lung cancer [7,8]. However, the mechanisms of $PM_{2.5}$-induced pulmonary injury is not fully understood.

The lung is characterized by the presence of a complex pattern of lipids, including phospholipids, cholesterol and sphingolipids, which play an important role in multiple physiologic and pathophysiologic processes. Phospholipids are the major composition of pulmonary surfactant, reducing the surface tension of the alveolus [9]. Lysophospholipids and oxidative phospholipids in the lung are increased in pulmonary inflammation and participate in the pathogenesis of pneumonia, asthma and lung fibrosis [10–12]. Cholesterol promotes the spreading, mobility and adsorption of pulmonary surfactant, but excess cholesterol impairs the surface tension reducing function [13,14]. Additionally, an increased number of cholesterol-overloaded macrophages

* Corresponding authors.
E-mail addresses: whuang@bjmu.edu.cn (W. Huang), xwang@bjmu.edu.cn (X. Wang).
[1] These authors contributed equally to this work.

http://dx.doi.org/10.1016/j.redox.2017.07.001
Received 5 January 2017; Received in revised form 26 June 2017; Accepted 2 July 2017
Available online 04 July 2017

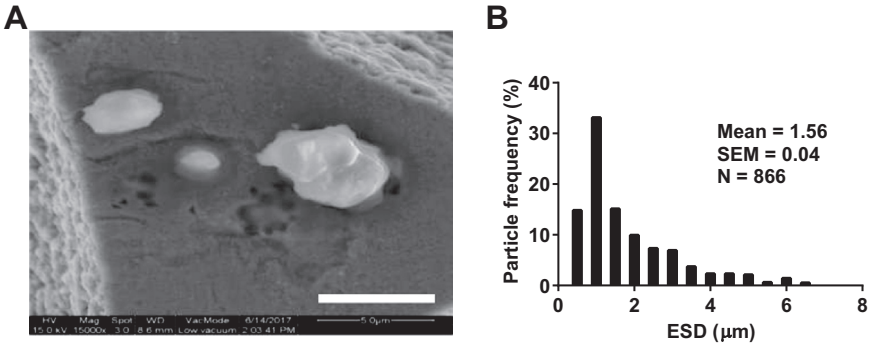

Fig. 1. $PM_{2.5}$ physical characteristics. (A) Representative scanning electron micrograph of $PM_{2.5}$ (Bar, 5 μm). (B) ESD distribution of $PM_{2.5}$. The data, including particle count and area, was measured by Image-J software and ESD was calculated.

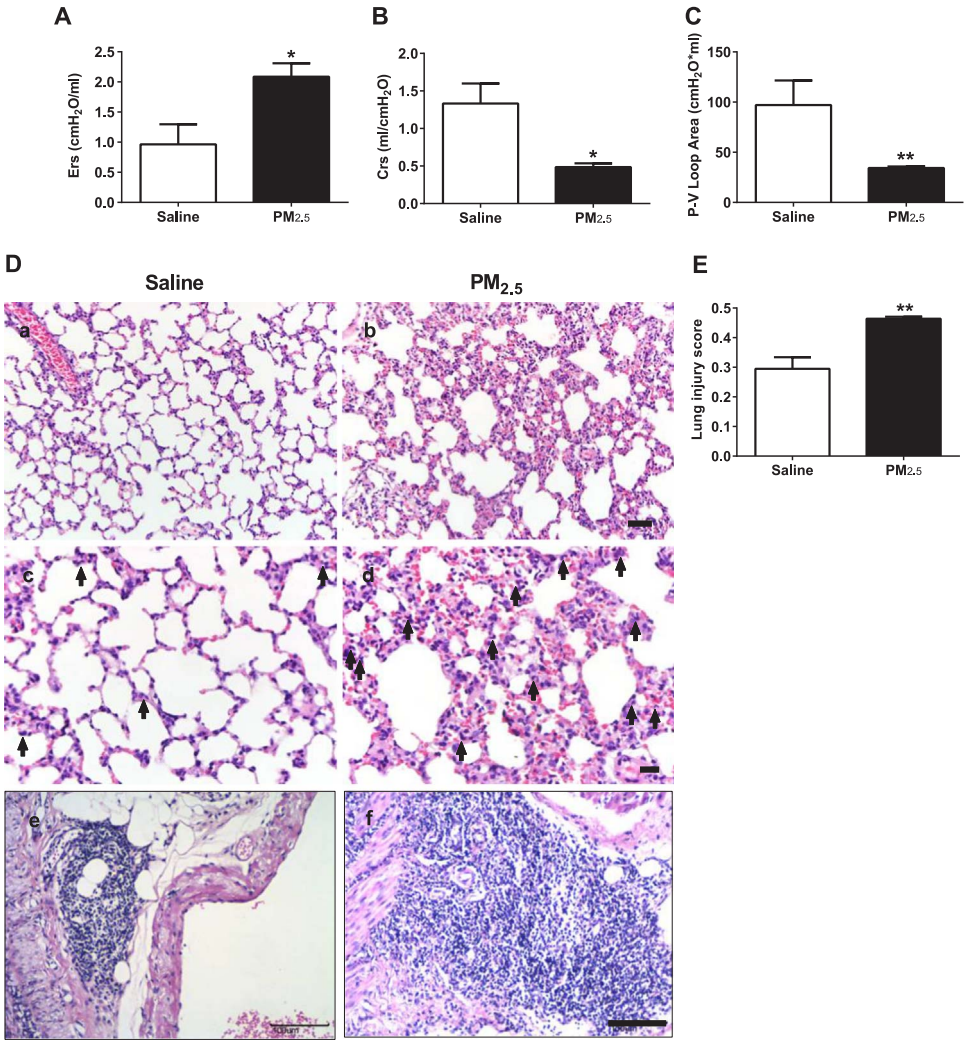

Fig. 2. Intra-tracheal instillation of $PM_{2.5}$ induces acute pulmonary injury. (A) Elasticity of the respiratory system (Ers) of rats. (B) Compliance of the respiratory system (Crs) of rats. (C) Area of the P-V loop of rats. (D) Representative H.E. staining of pulmonary tissue of rats (Bars, a, b: 50 μm, c, d: 20 μm, e, f: 100 μm; Arrow, PMNs). (E) Lung injury score of rats. $PM_{2.5}$ (45 mg/kg) was intra-tracheally instilled into rats on the 1st, 3rd and 6th days (n = 3–5). (A-C, E) All of the data are presented as the means ± SEM. Two-tailed Student's t-test: * $P < 0.05$, ** $P < 0.01$ compared with the saline instillation group.

has been observed in pneumonia, lung fibrosis and lung cancer, promoting the onset of these diseases [10]. Ceramide (Cer), a sphingolipid metabolite, induces the apoptosis of alveolar epithelial cells and the formation of the alveolus, while sphingosine-1-phosphate (S1P) maintains the survival of cells, which are important for the structural and functional development of the lung [15]. The imbalance of Cer and S1P leads to alveolar enlargement or fibrosis and is involved in the onset of COPD, asthma, lung fibrosis and lung cancer [16]. Although a phospholipid metabolism profile of pulmonary tissue after $PM_{2.5}$ exposure has been carried out [17], the global lipid metabolism change induced by $PM_{2.5}$ is largely unknown.

In this study, $PM_{2.5}$ was given to rats through intra-tracheal instillation *in vivo*, and metabolomics were utilized to delineate the lipid metabolic profile in broncho-alveolar lavage fluid (BALF). $PM_{2.5}$ activated the metabolism of phospholipids and sphingolipids. Next, benzo [a]pyrene (BaP), a compound belonging to polycyclic aromatic hydrocarbon (PAH), was found to be enriched in $PM_{2.5}$. A human alveolar type II cell line, A549, was employed and treated with BaP. BaP induced inflammation in A549 cells. The metabolomics results revealed that BaP promoted the metabolism of phospholipids, sphingolipids and free fatty acids (FFAs), indicating the increase in phospholipase A2 (PLA2) activity. Mechanically, BaP increased the activity of PLA2 in a Ca^{2+}-dependent manner, mediating inflammation.

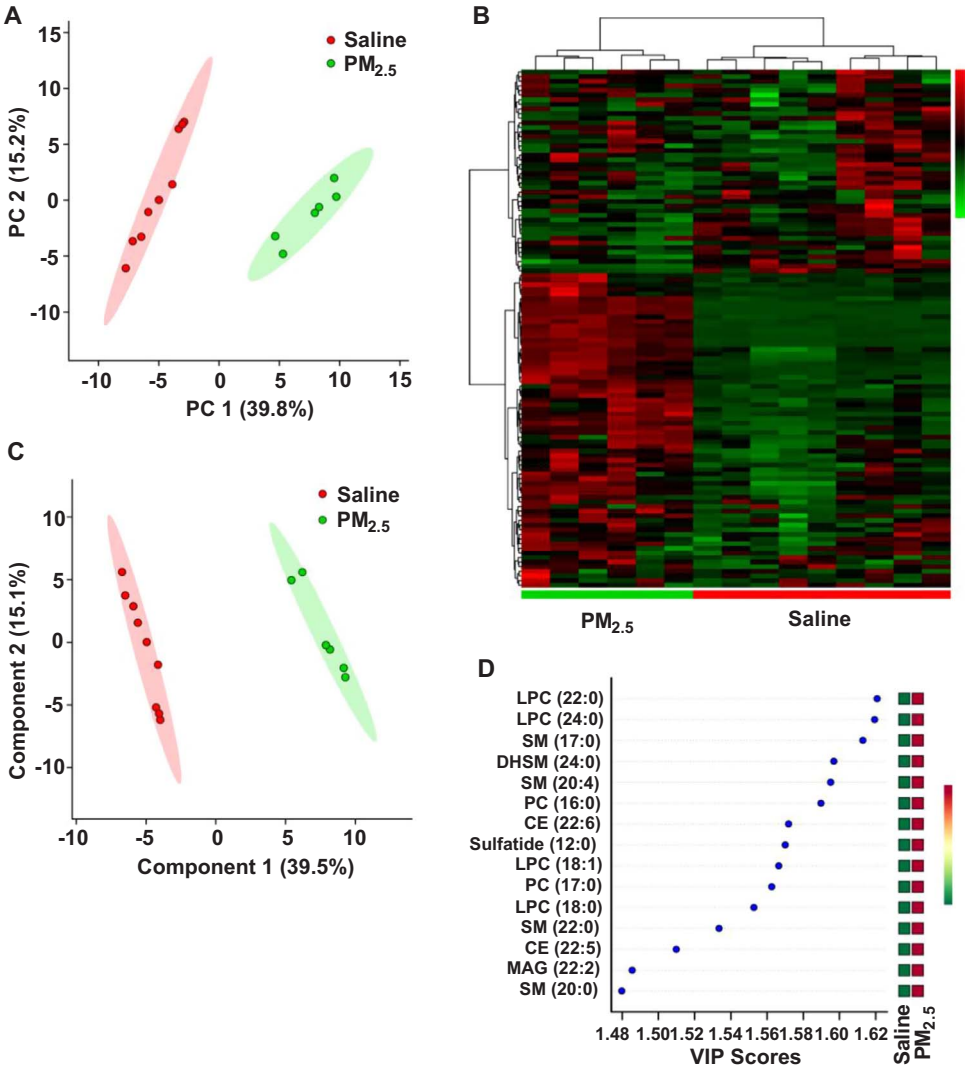

Fig. 3. Intra-tracheal instillation of $PM_{2.5}$ alters lipid metabolism in the lung. (A) PCA scatter plot of the lipid metabolites from BALF. (B) Heat map of the lipid metabolic profile from BALF. (C) PLS-DA scatter plot of the lipid metabolites from BALF. (D) VIP score plot of the lipid metabolites from BALF. $PM_{2.5}$ (45 mg/kg) was intra-tracheally instilled into rats on the 1st, 3rd and 6th days (n = 3–5).

2. Materials and methods

2.1. Reagents

The anti-NOS2 antibody was purchased from Santa Cruz Biotechnology (Santa Cruz, CA, USA). The anti-β-actin antibody was purchased from Cell Signaling Technology (Boston, MA, USA). BaP was purchased from Sigma-Aldrich Chemical (St. Louis, MO, USA). The phospholipase A2 assay kit was purchased from Thermo Fisher Scientific (Waltham, MA, USA).

2.2. $PM_{2.5}$ sampling and preparation

$PM_{2.5}$ samples were collected in March 2015 in Beijing, China for use in the present study. The $PM_{2.5}$ samples were collected onto the fiber filters using a particulate sampler. The filters were weighed and cut into squares of 1–2 cm^2. The particulate matter in the samples was removed by agitation in ultrapure water with an ultrasonic shaker. The solution was frozen and dried using a vacuum freeze dryer. The dried $PM_{2.5}$ was weighed and kept at −20 °C before being diluted for the experiments.

2.3. Scanning electron microscopy

Size distribution of PM was measured by a field emission environmental scanning electron microscopy. Particle size was determined by Image-J software. Scanning electron microscopy was digitized and particle area measurements were made. The equivalent spherical diameter (ESD), a commonly used parameter for particle sizing, was calculated using the formula: $ESD = 2 \times (area / \pi)^{1/2}$ [18].

2.4. Animals

Male Wistar rats (180–220 g) were housed in a temperature-controlled room (22 °C) with a 12-h light/dark cycle and free access to laboratory chow and tap water. All of the animal protocols followed the "National Institutes of Health guide for the care and use of laboratory animals" and were approved by the Animal Care and Use Committee of Peking University.

2.5. Broncho-alveolar $PM_{2.5}$ instillation and lavage

Before the experiments, $PM_{2.5}$ was diluted in sterile saline at a concentration of 15 mg/ml. The rats were anesthetized and were instilled with sterile saline or $PM_{2.5}$ at a volume of 3 ml/kg into the bronchus on the first day. The intra-tracheal instillation was repeated another two times on the 3rd and 6th days. Twenty-four hours after the last intra-tracheal instillation, the rats were anesthetized. The pulmonary functional variables were then measured by flexiVent (SCIREQ, Montreal, QC, Canada). The rats were sacrificed; immediately after death, the left lung was ligated, and the trachea to the left lung was cannulated. The right lung was douched with 3 ml sterile saline for

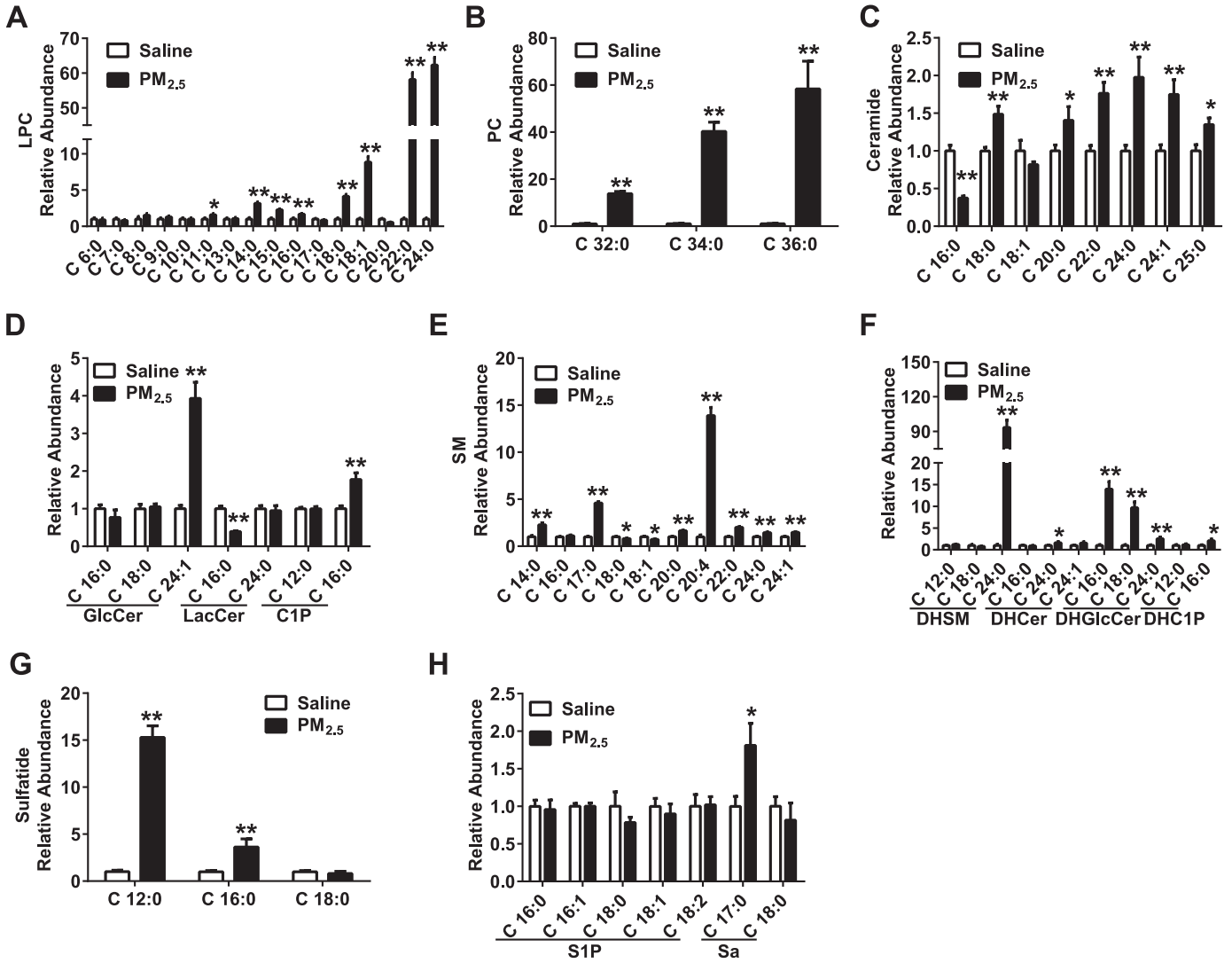

Fig. 4. Intra-tracheal instillation of $PM_{2.5}$ activates phospholipid and sphingolipid metabolism in the lung (A-H) Levels of LPC (A), PC (B), ceramide (C), GlucoCer, LactoCer, C1P (D), SM (E), DHSM, DHCer, DHGlucoCer, DHC1P (F), sulfatide (G) and S1P (H) in BALF. $PM_{2.5}$ (45 mg/kg) was intra-tracheally instilled into rats on the 1st, 3rd and 6th days (n = 3–5). All of the data are presented as the means ± SEM. Two-tailed Student's t-test: * $P < 0.05$, ** $P < 0.01$ compared with the saline instillation group.

three times. The lavage fluid was centrifuged and stored at −80 °C.

2.6. Histologic assessment

The lung were harvested and fixed in buffered formaldehyde after lavage. The fixed lung were embedded in paraffin and performed the hematoxylin and eosin (H.E.) staining for light microscopy. The infiltration of polymorphonuclear neutrophils (PMNs) were counted. The lung injury score was calculated on high-power field as described [19].

2.7. Sample preparation for metabolomics analysis

To prepare BALF, 200 µl of BALF was extracted by 4-fold cold chloroform/methanol (2/1) containing Cer (19:0) (5 nM) as the lipid metabolite internal standard. For the cells, the pellets were resuspended in 100 µl of saline and were extracted in the same way as BALF. The extractions were vortexed and centrifuged. The lower organic phase and upper hydrophilic phase were collected and evaporated, respectively. The organic residue was dissolved in 50 µl of chloroform/methanol (1/1). The samples were centrifuged at 18,000 rpm for 20 min, and 5 µl was injected into the ultra-performance liquid chromatography tandem mass spectrometry (UPLC-MS/MS) system.

2.8. Metabolomics detection by UPLC-MS/MS

Metabolites were identified and quantified by a UPLC (Waters, Milford, MA, USA) interfaced to a 5500 QTRAP hybrid triplequadruple linear ion-trap MS (AB Sciex, Foster City, CA, USA) outfitted with a turbo ion-spray ionization source.

Hydrophilic analytes were separated using a Waters Amide XBridge HPLC column (3.5 µm; 4.6 mm inner diameter * 100 mm length) (Waters, Milford, MA, USA) maintained at 30 °C. The mobile phase was water containing 5 mM ammonium acetate (A) and methanol (B). The gradient was as follows: 0–3 min 90% B, 3–15 min 90–40% B, 15–16 min 40–2% B, 16–18 min 2% B, 18–19 min 2–90% B, and 19–23 min 90% B. The flow rate was 0.5 ml/min.

Lipid analytes were separated using a Waters ACQUITY UPLC CSH C18 Column (130 Å, 1.7 µm, 2.1 mm × 100 mm, 1/pkgCSH) (Waters, Milford, MA, USA) maintained at 55 °C. Mobile phase was methanol/water/ acetonitrile of 1/1/1 containing 5 mM ammonium acetate (A) and isopropanol (B). The gradient was as follows: 0–0.5 min 20% B, 0.5–1.5 min 20–40% B, 3 min 60% B, 13 min 98% B, and 13.2–17 min 20% B. The flow rate was 0.3 ml/min.

The response curves were calculated using MultiQuant software. Principal component analysis (PCA), partial least squares discriminant analysis (PLS-DA), variable importance for the projection (VIP) score,

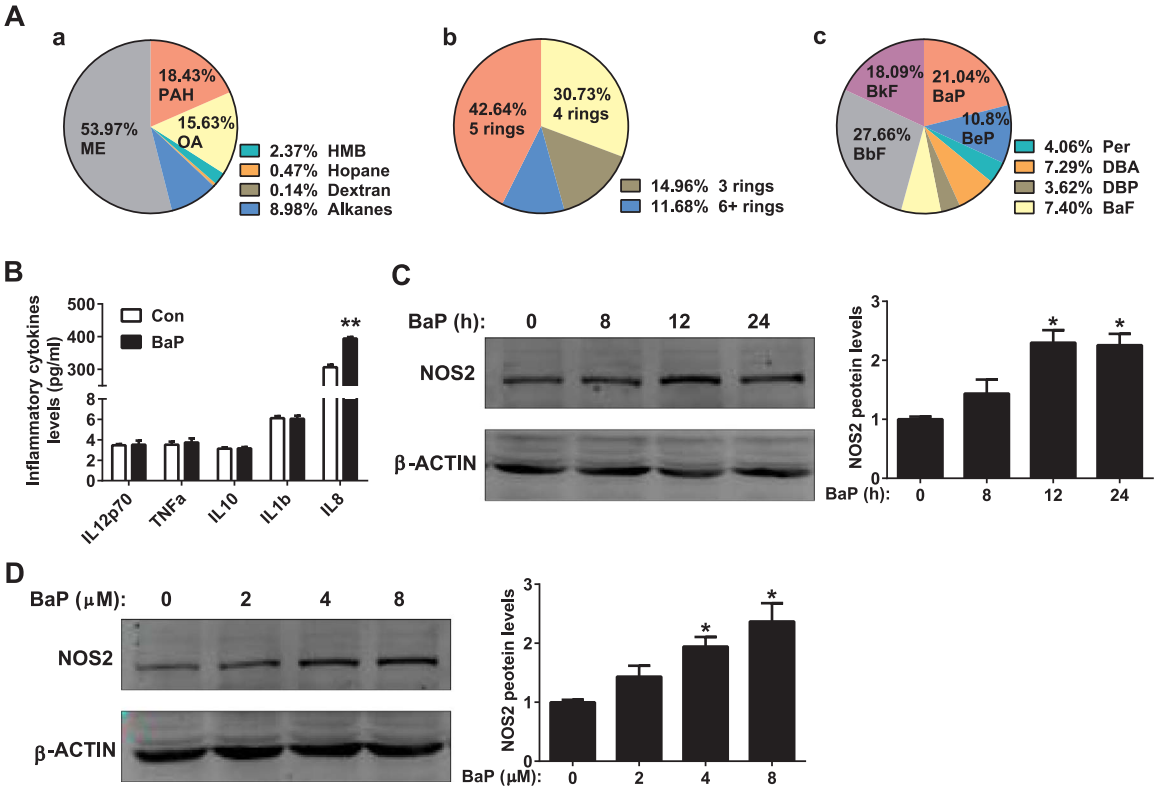

Fig. 5. BaP promotes inflammation in alveolar type II cells. (A) Organic tracer analysis of $PM_{2.5}$. (B) Levels of inflammatory cytokines in the supernatants of A549 cells. The A549 cells were treated with control or BaP (4 μM) for 24 h ($n = 6$). (C) Western blot analysis (right panel) and quantitation (left panel) of NOS2 protein in A549 cells. A549 cells were treated with control or BaP (4 μM) for the indicated hours ($n = 3$). (D) Western blot analysis (right panel) and quantitation (left panel) of NOS2 protein in A549 cells. A549 cells were treated with control or the indicated doses of BaP for 24 h ($n = 3$). All of the data are presented as the means ± SEM. (B) Two-tailed Student's *t*-test: * $P < 0.05$, ** $P < 0.01$ compared with the control group. (C, D) One-way ANOVA with Tukey's correction: * $P < 0.05$ compared with the control group.

unsupervised hierarchical clustering analysis, scatter plots and heatmap generation were carried out using MetaboAnalyst 3.0 (http://www.metaboanalyst.ca/).

2.9. Cytometric bead array

The supernatant inflammatory cytokine levels were investigated using a cytometric bead array inflammation kit (BD Biosciences, San Jose, CA, USA) and were analyzed by BD FACSCalibur (BD Biosciences, San Jose, CA, USA) with Cell QuestPro software.

2.10. Measurement of the free intracellular Ca^{2+} concentration

The A549 cells were cultured in 96-well plates and were washed once with phosphate-buffered saline. Next, Hank's balanced salt solution (HBSS) with Fluo3-AM (Bio-Rad Laboratories, Hercules, CA, USA) was added to the cells and was incubated for 30 min at 37 °C in a 5% CO_2 atmosphere. The cells were washed once with HBSS, which was replaced with HBSS containing DMSO or BaP. The fluorescence of Ca^{2+}/Fluo3 was monitored over time. F_{max} was measured with Fluo3-AM-preloaded cells treated with 0.1% Triton X-100, and F_{min} was measured with Fluo3-AM-preloaded cell-free wells. $[Ca^{2+}]$ was calculated using the formula: $[Ca^{2+}] = K_d \times (F\text{-}F_{min}) / (F_{max}\text{-}F)$. The dissociation constant (K_d) of Fluo3 was assumed to be 400 nM.

2.11. Western blot analysis

Proteins were subjected to SDS-PAGE with a 12% running gel and were then transferred to a polyvinylidene fluoride membrane. The membrane was incubated successively with 0.1% bovine serum albumin in Tris/Tween-20-buffered saline at room temperature for 1 h, with different antibodies at 4 °C for 12 h and then with second antibody for 1 h. The immunofluorescence bands were detected by the Odyssey infrared imaging system (LI-COR Biosciences, Lincoln, NE, USA).

2.12. qPCR analysis

Total RNA was isolated using Trizol reagent (Promega, Madison, WI, USA). Total RNA (2 μg) was reverse transcribed using a reverse transcription system (Promega, Madison, WI, USA). Next, 4 μl of the reaction mixture was included in the PCR samples with the Mx3000 Multiplex Quantitative PCR System (Agilent, La Jolla, CA, USA). The amount of the PCR products formed in each cycle was evaluated using SYBR Green I fluorescence. The results were analyzed using the Stratagene Mx3000 software, and the target mRNA levels were normalized to the levels of β-actin.

2.13. Statistical analysis

The data were analyzed using GraphPad Prism software and were expressed as the means ± SEM. Unpaired Student's *t*-test and one-way ANOVA with Tukey's correction were used as appropriate. $P < 0.05$ was considered significant.

3. Results

3.1. $PM_{2.5}$ physical characteristics

The morphology of PM, isolated from the fiber filters, was firstly analyzed by scanning electron microscopy. The PM displayed various size and shape (Fig. 1A). The mean ESD of the PM was 1.56 ± 0.04 μm and the ESD distribution of the PM was also shown (Fig. 1B). Over 80% of the PMs had an ESD less than 2.5 μM and the PMs that had an ESD over 2.5 μM might be due to the aggregation of small PMs. Therefore,

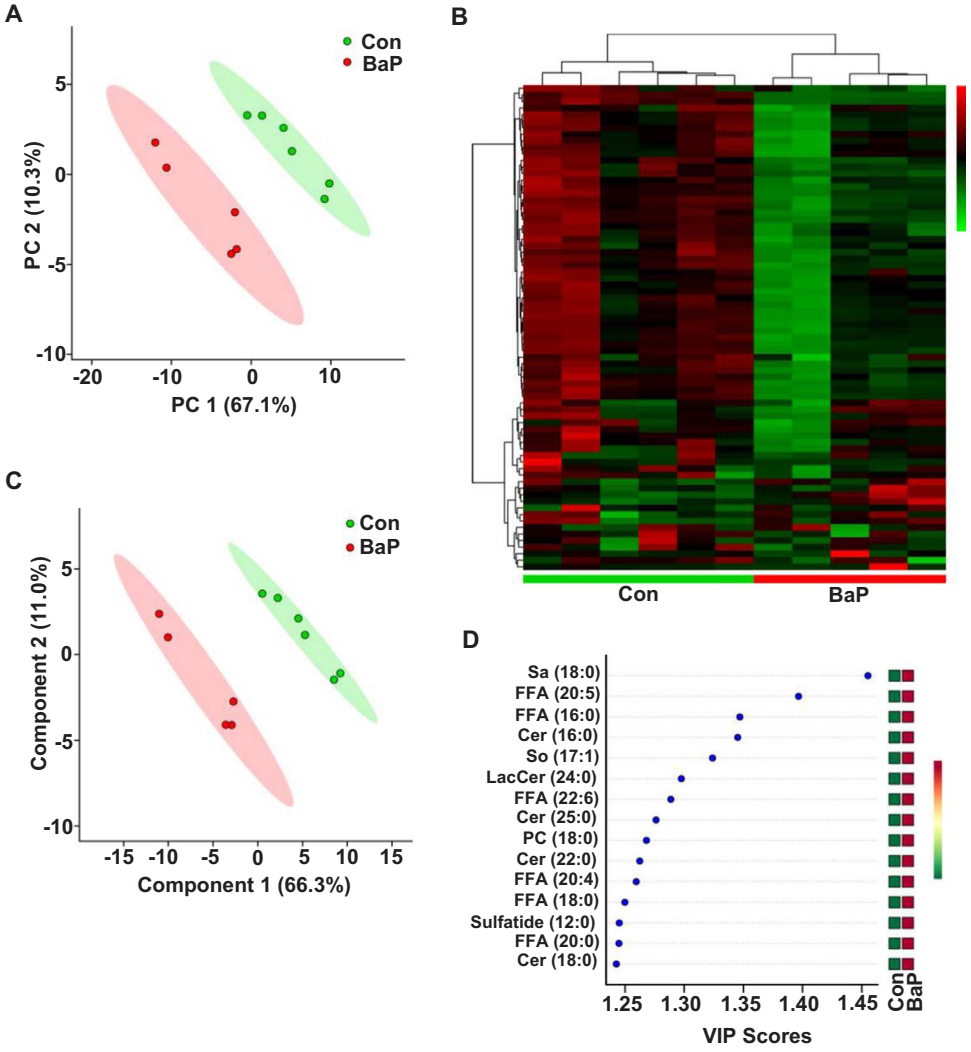

Fig. 6. BaP alters sphingolipid and FFA metabolism in alveolar type II cells. (A) PCA scatter plot of the lipid metabolites in A549 cells. (B) Heat map of the lipid metabolic profile in A549 cells. (C) PLS-DA scatter plot of the lipid metabolites in A549 cells. (D) VIP score plot of the lipid metabolic profile in A549 cells. A549 cells were treated with control or BaP (4 μM) for 6 h (n = 5–6).

the PMs, used in the experiments, are $PM_{2.5}$.

3.2. Intra-tracheal instillation of $PM_{2.5}$ induces acute pulmonary injury

$PM_{2.5}$, collected from the fiber filters, was instilled to the broncho-alveolar system of Wistar rats. The instillation was performed on the 1st, 3rd, and 6th days 3 times in total. The body weight of the rats increased during the period of instillations and was not affected by $PM_{2.5}$ (45 mg/kg) (Supplementary Fig. 1A), revealing that the instillation did not cause systemic harm to the rats.

Twenty-four hours after the last instillation, the pulmonary function was examined. The inspiratory capacity (IC) and resistance of the respiratory system (Rrs) were not changed (Supplementary Fig. 1B, C). However, the elasticity of the respiratory system (Ers) was increased (Fig. 2A), and the compliance of the respiratory system (Crs) was decreased compared with those in the saline group (Fig. 2B). In addition, the area of the Pressure-Volume (P-V) loop was reduced after the instillation of $PM_{2.5}$ (Fig. 2C), suggesting the impaired pulmonary function.

Furthermore, the histological changes of the lung was examined by H.E. staining after instillation. The intra-tracheal administration of $PM_{2.5}$ thickened the alveolar wall (Fig. 2D: a, b) and induced the exudation and infiltration of PMNs (Fig. 2D: c, d), which was consistent with the changes in pulmonary function. The hilar lymph nodes were also enlarged after $PM_{2.5}$ instillation (Fig. 2D: e, f). Then, a combined lung injury score was generated and revealed an increased lung injury score in the $PM_{2.5}$ group (Fig. 2E). These results indicate that $PM_{2.5}$ induced acute pulmonary injury and inflammation in rats.

3.3. Intra-tracheal instillation of $PM_{2.5}$ altered lipid metabolism in the lung

To examine the $PM_{2.5}$-induced pulmonary metabolomics change, BALF from the rats receiving broncho-alveolar instillation was collected and was analyzed by UPLC-MS/MS. In general, 124 distinct lipid metabolites were identified and 33 of these metabolites were changed significantly ($P < 0.05$, fold change (FC) > 2) (Supplementary Table 1).

The BALF from rats instilled with $PM_{2.5}$ displayed a different lipid metabolic profile from that of the saline instilled rats, according to the PCA plot (Fig. 3A). The heatmap also showed a clustering of lipid metabolites between the $PM_{2.5}$ and saline groups (Fig. 3B). The PLS-DA plot and VIP score plot revealed that the phospholipid metabolism: lysophosphatidylcholine (LPC) (18:0, 18:1, 22:0, 24:0) and phosphatidylcholine (PC) (16:0, 17:0, 18:0) and the sphingolipid metabolism: sphingomyelin (SM) (17:0, 20:0, 20:4, 24:0), dihydrosphingomyelin (DHSM) (24:0), and sulfatide (12:0) had higher VIP values (Fig. 3C, D).

3.4. Intra-tracheal instillation of $PM_{2.5}$ activates phospholipid and sphingolipid metabolism in the lung

Next, metabolite changes in phospholipids and sphingolipids were examined. The levels of phospholipid metabolites, including LPC (11:0, 14:0, 15:0, 18:0, 18:1, 22:0, 24:0) (Fig. 4A) and PC (32:0, 34:0, 36:0)

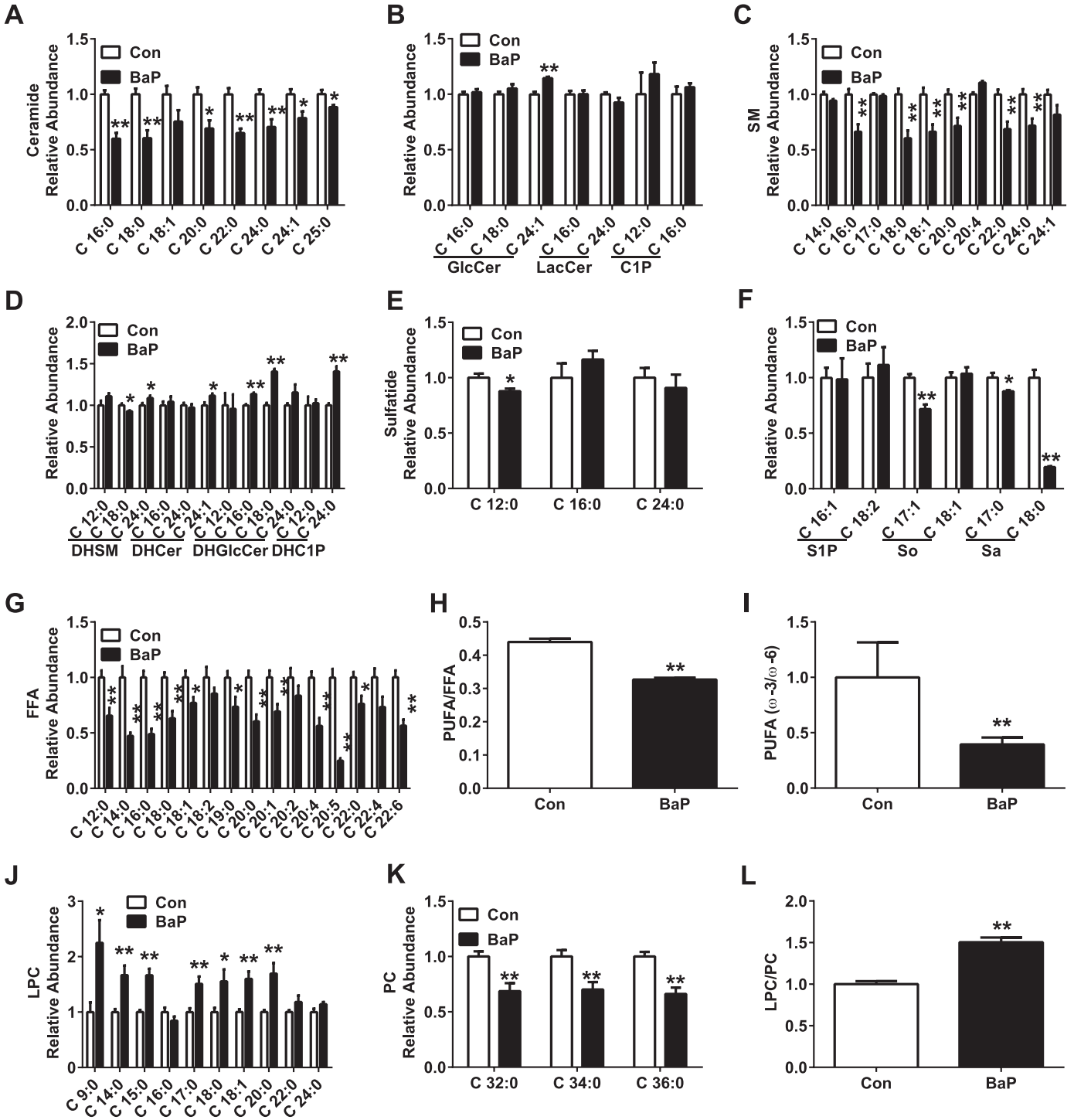

Fig. 7. BaP activates sphingolipid, FFA and phospholipid metabolism in alveolar type II cells. (A-G) Levels of Cer (A), GlcCer, LacCer, C1P (B), SM (C), DHSM, DHCer, DHGlcCer, DHC1P (D), Sulfatide (E), S1P, So, Sa (F), and FFA (G) in A549 cells. (H, I) Ratios for PUFA/FFA (H) and ω–3/ω–6 PUFA (I) in A549 cells. (J, K) Levels of LPC (J), and PC (K) in A549 cells. (L) Ratio for LPC/PC in A549 cells. A549 cells were treated with control or BaP (4 μM) for 6 h (n = 5–6). All of the data are presented as the means ± SEM. Two-tailed Student's t-test: * $P < 0.05$, ** $P < 0.01$ compared with the control group.

(Fig. 4B), were increased in the BALF after the instillation of $PM_{2.5}$.

Additionally, the levels of sphingolipid metabolites, including Cer (18:0, 20:0, 22:0, 24:0, 24:1, 25:0) (Fig. 4C), glucosylceramide (GlcCer) (24:1), ceramide-1-phosphate (C1P) (16:0) (Fig. 4D), SM (14:0, 17:0, 20:0, 20:4, 22:0, 24:0, 24:1) (Fig. 4E), DHSM (24:0), dihydroceramide (DHCer) (24:0), dihydroglucosylceramide (DHGlcCer) (16:0, 18:0, 24:0), dihydroceramide-1-phosphate (DHC1P) (16:0) (Fig. 4F), sulfatide (12:0, 16:0) (Fig. 4G) and sphinganine (Sa) (17:0) (Fig. 4H), were increased in the BALF of $PM_{2.5}$ treated rats. However, the levels of Cer (16:0) (Fig. 4C), lactosylceramide (LacCer) (16:0) (Fig. 4D) and SM (18:0, 18:1) (Fig. 4E) were decreased in the $PM_{2.5}$ group. These results suggest an increased metabolism of phospholipids and sphingolipids in response to $PM_{2.5}$ instillation in the rat lung.

A series of results showed that both phospholipids and sphingolipids played an important role in pulmonary inflammation. Bioactive LPC levels were increased at the sites of inflammation, promoting chemotaxis, adherence, differentiation, activation and cytokine secretion of immune cells in the lung [11]. Cer was generated through the

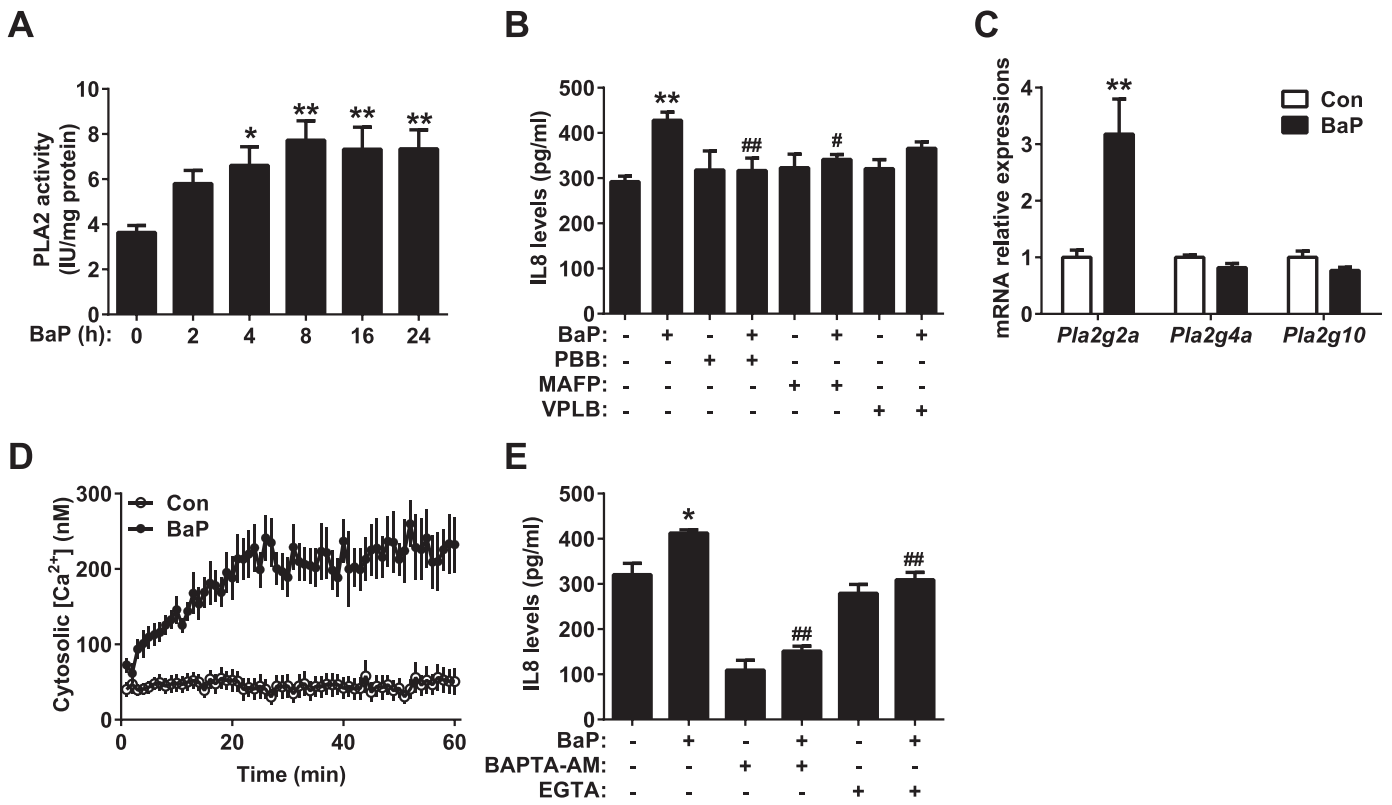

Fig. 8. Activation of PLA2 mediates BaP-induced inflammation in a Ca^{2+}-dependent manner. (A) Activity of PLA2 in A549 cells. The A549 cell lines were treated with control or BaP (4 μM) for the indicated hours ($n = 6$). (B) Levels of IL8 in the supernatants of A549 cells. After pretreatment with PBB (100 μM), MAFP (5 μM) or VPLB (3 μM) for 1 h, the A549 cells were treated with control or BaP (4 μM) for 24 h ($n = 6$). (C) The mRNA levels of *Pla2g2a*, *Pla2g4a* and *Pla2g10* in A549 cells. A549 cells were treated with control or BaP (4 μM) for 12 h ($n = 4$). (D) Intracellular Ca^{2+} level in A549 cells. After preloading with Fluo3-AM (3 μM) for 1 h, the A549 cells were treated with control or BaP (4 μM) for the indicated minutes ($n = 16$). (E) Levels of IL8 in the supernatants of A549 cells. After pretreatment with BAPTA-AM (50 μM) or EGTA (5 mM) for 1 h, the A549 cells were treated with control or BaP (4 μM) for 24 h ($n = 4$). All of the data are presented as the means ± SEM. (A, B, E) One-way ANOVA with Tukey's correction: * $P < 0.05$, ** $P < 0.01$ compared with the control group, # $P < 0.05$, ## $P < 0.01$ compared with the BaP treatment group. (C) Two-tailed Student's *t*-test: ** $P < 0.05$ compared with the control group.

upregulation of sphingomyelinase and promoted apoptosis, cytokine secretion, and decreased endothelial barrier integrity in the lung [16]. As a result, the activation of phospholipid and sphingolipid metabolism may participate in $PM_{2.5}$-induced pulmonary inflammation and injury.

3.5. BaP promotes the inflammation in alveolar type II cells

To determine the exact component that is responsible for inflammation and pulmonary injury, $PM_{2.5}$ was extracted from fiber filters, and the organic components were examined. PAHs were the most toxic components and were relatively enriched in $PM_{2.5}$ (Fig. 5A: a). Further analysis revealed that 4-ring and 5-ring PAHs occupied the largest percentages of the PAHs in $PM_{2.5}$ (Fig. 5A: b). BaP was one of the most abundant components in 5-ring PAHs (Fig. 4A: c) and was the most toxic compound among the 4-ring and 5-ring PAHs [20]. Therefore, BaP was employed to treat a human alveolar type II cell line, A549, *in vitro*.

The pro-inflammatory effect of BaP was examined first in A549 cells. BaP (4 μM) treatment for 24 h increased the supernatant level of IL8, a pro-inflammatory chemokine (Fig. 5B), while the levels of IL12, TNFα, IL10 and IL1β remained unchanged (Fig. 5B). The expression of NO synthase 2 (NOS2) was increased after pro-inflammatory stimulus treatment, generating NO to mediate inflammation [21]. BaP (2–8 μM) up regulated the expression of NOS2 in a time- and dose-dependent manner (Fig. 5C, D). These results indicate that BaP induced inflammation in alveolar type II cells.

3.6. BaP alters sphingolipid and FFA metabolism in alveolar type II cells

To investigate whether BaP altered lipid metabolism, A549 cells were treated with BaP (4 μM) for 6 h and underwent UPLC-MS/MS. In general, 79 distinct lipid metabolites were identified, and 25 of these metabolites were changed significantly ($P < 0.05$, FC > 1.5) (Supplementary Table 2).

The PCA plot displayed a disparate lipid metabolic profile in A549 cells after BaP treatment (Fig. 6A). Heatmap and cluster analysis witnessed good differentiation in metabolomics, clustering in A549 cells with or without BaP treatment (Fig. 6B). The PLS-DA and VIP score plots were further applied to choose the important variables. The score showed the change in the metabolic profile converged largely on sphingolipid metabolism: Sa (18:0), Cer (16:0, 18:0, 22:0, 25:0), sphingosine (So) (17:1), LacCer (24:0), sulfatide (12:0) and FFA (16:0, 18:0, 20:0, 20:4, 20:5, 22:6) (Fig. 6C, D).

3.7. BaP activates sphingolipid, FFA and phospholipid metabolism in alveolar type II cells

BaP decreased the levels of Cer (16:0, 18:0, 20:0, 22:0, 24:0, 24:1, 25:0) (Fig. 7A), SM (16:0, 18:0, 18:1, 20:0, 22:0, 24:0) (Fig. 7C), DHSM (18:0) (Fig. 7D), sulfatide (Fig. 7E), So (17:1) and Sa (17:0, 18:0) (Fig. 7F), but BaP increased the levels of GlcCer (24:1), DHSM (24:0), DHCer (24:1), DHGlcCer (16:0, 18:0) and DHC1P (24:0) in A549 cells (Fig. 7F); these results partially contrast with the results from the *in vivo* experiments.

The levels of FFA were examined. BaP treatment decreased the levels of different species of FFA (12:0, 14:0, 16:0, 18:0, 18:1, 19:0, 20:0, 20:1, 20:4, 20:5, 22:0, and 22:6) in A549 cells (Fig. 7G), especially the proportion of polyunsaturated fatty acid (PUFA) (Fig. 7H). Within the different species of PUFA, the ratio of ω–3/ω–6 PUFA was also decreased (Fig. 7I), suggesting that the anti-inflammatory effect driven by

ω–3 PUFA was decreased after BaP treatment.

Phospholipids are the major component of pulmonary surfactant secreted by alveolar type II cells and are involved in pulmonary inflammation [22]. In addition, there was a marked change in phospholipids in the BALF of rats after $PM_{2.5}$ instillation *in vivo* (Fig. 3D). Therefore, the change in phospholipids after BaP treatment was also examined. The levels of LPC (9:0, 14:0, 15:0, 17:0, 18:0, 18:1, and 20:0) were increased after BaP treatment in A549 cells (Fig. 7J), which was in line with the results from the *in vivo* experiments. However, the levels of PC (32:0, 34:0, and 36:0) was decreased (Fig. 7K), suggesting the dysfunction of pulmonary surfactant generation. The hydrolysis of PC to LPC depends on phospholipase A2 (PLA2) [23]. BaP treatment markedly decreased the ratio of LPC/PC (Fig. 7L), suggesting the increased activity of PLA2 in these cells.

3.8. The activation of PLA2 mediates BaP-induced inflammation in a Ca^{2+}-dependent manner

PLA2 catalyzes the hydrolysis of the *sn*-2 position of glycerophospholipid to liberate lysophospholipid and FFA [11]. To determine whether PLA2 was involved in BaP-induced inflammation in A549 cells, PLA2 activity was first examined. BaP increased the activity of total PLA2, as early as 4 h, in a time-dependent manner, in A549 cells (Fig. 8A). PLA2 was mainly classified into three families: cytosolic PLA2 (cPLA2), Ca^{2+}-independent PLA2 (iPLA2) and secretory PLA2 (sPLA2) [24]. Different inhibitors were added to A549 cells to distinguish different subtypes of PLA2. The BaP-induced secretion of IL8 was partially reversed by *p*-bromophenacyl bromide (PBB), a general PLA2 inhibitor and methyl arachidonyl fluorophosphonate (MAFP), a cPLA2 and iPLA2 inhibitor (Fig. 8B). Varespladib (VPLB), a sPLA2 inhibitor, had only a mild inhibitory effect on IL8 secretion and was not statistically significant (Fig. 7B), indicating that cPLA2 or iPLA2 contributed most to the inflammation induced by BaP in the A549 cells.

Next, the expression of PLA2 in A549 cells was further examined. BaP up regulated the mRNA level of *Pla2g2a*, a sPLA2 gene. However, the expression of *Pla2g4a* and *Pla2g10* remained unchanged (Fig. 8C). In addition, the upregulation of *Pla2g2a* occurred posterior to increased PLA2 activity (Supplementary Fig. 2A-C), suggesting that the increased PLA2 activity was due to the activation, not the expression, of PLA2. The activation of cPLA2 depends on Ca^{2+}. BaP was found to increase intracellular Ca^{2+} in A549 cells (Fig. 8D). To determine whether the BaP-induced activation of PLA2 depended on Ca^{2+}, different Ca^{2+} chelators were added to A549 cells. The BaP-induced IL8 secretion was partially inhibited by BAPTA-AM, an intracellular Ca^{2+} chelator, and EGTA, an extracellular Ca^{2+} chelator (Fig. 8E), suggesting that BaP induces inflammation by increasing extracellular Ca^{2+} influx in A549 cells.

4. Discussion

In this study, metabolomics was employed to examine the lipid profile of $PM_{2.5}$-induced pulmonary injury. $PM_{2.5}$ was given to rats through intra-tracheal instillation *in vivo*. $PM_{2.5}$ impaired pulmonary function and induced pulmonary inflammation. Metabolomics analysis revealed increased metabolism of phospholipids and sphingolipids in the BALF of $PM_{2.5}$-treated rats. BaP was one of the most abundant pollutants in $PM_{2.5}$ particles. To explore the mechanisms, A549 cells, a human alveolar type II cell line, were employed and treated with BaP. BaP promoted inflammation in A549 cells and activated the metabolism of phospholipids, sphingolipids and FFAs. BaP increased the activity of PLA2. BaP-induced inflammation was reversed by general PLA2 and cPLA2 inhibitors. BaP mainly activated cPLA2 and promoted LPC generation by elevating intracellular Ca^{2+}, promoting inflammation.

Previous studies have reported that acute exposure to low dose $PM_{2.5}$ induces inflammation, oxidative stress and impairment of pulmonary function [25,26]. In consistent with previous studies, intra-tracheal instillation of $PM_{2.5}$ induced acute pulmonary injury, indicated by higher lung injury score. The increased infiltration of neutrophils into the interstitium was observed after $PM_{2.5}$ instillation, which is considered to play a vital role in the acute pulmonary injury [27]. $PM_{2.5}$ has been reported to induce the production of reactive oxygen species in neutrophils of asthmatic patients, which is involved in neutrophil activation and pulmonary injury [28]. The expression of adhesion molecules in endothelium is also up regulated after treatment of $PM_{2.5}$ [29,30], facilitating the migration of neutrophils into the lung.

$PM_{2.5}$ promotes the expression and secretion of IL8 [31], which is a powerful chemokines to neutrophils and has been shown to play an important role in the onset of airway inflammation [32]. BaP increases the secretion of pro-inflammatory cytokines, including IL8, inducing pulmonary inflammation [33–36]. In accordance with previous studies, the secretion of IL8 was increased in A549 cells by BaP. As BaP is one of the components of $PM_{2.5}$, BaP-induced IL8 secretion may be involved in the infiltration of neutrophils in the lung after $PM_{2.5}$ instillation.

The detrimental effect of $PM_{2.5}$ on the body is closely associated with lipid metabolism. Long-term $PM_{2.5}$ exposure has been shown to accelerate the pathogenesis of lipid-associated metabolic disease, including atherosclerosis and type II diabetes [37,38], by inducing dyslipidemia [39,40], vascular inflammation [37], adipose dysfunction [41,42] and insulin resistance [38]. The lipid metabolic profile of plasma has been delineated after the exposure of $PM_{2.5}$ [43,44]. However, as the first barrier following exposure to a high level of $PM_{2.5}$, pulmonary global lipid metabolomics has not been carefully studied. In this study, the metabolomics of both BALF from rats instilled with $PM_{2.5}$ *in vivo* and A549 cells treated with BaP were examined.

The metabolomics profile revealed that $PM_{2.5}$ instillation mainly increased LPC and PC levels in BALF. However, another study found that $PM_{2.5}$ decreased the levels of these metabolites in pulmonary tissue [17]. In that study, $PM_{2.5}$ was given to rats through ambient air for 8 months and histopathology revealed emphysema [17]; however, in our study, $PM_{2.5}$ was given to rats through acute instillation, and histopathology only exhibited edema and infiltration of PMNs in the alveolar septum, which is a different stage of $PM_{2.5}$-induced pulmonary injury. In the early stage of pulmonary injury, the elevation of LPC and PC levels was a response to $PM_{2.5}$ stimulation. In the late stage, however, the LPC and PC levels might be decreased due to decompensation. This contradiction displayed a dynamic change in the pulmonary lipid profile in different stages of $PM_{2.5}$-induced pulmonary injury.

In the lung, the alveolar epithelium consists of type I and type II epithelial cells. Alveolar type II cells occupy about 4% of the alveolar surface but play an important role in maintaining the normal structure and function of the alveolus. Alveolar type II cells can trans-differentiate into alveolar type I cells to repair the alveolus and secrete cytokines to induce pulmonary inflammation [22,45–47]. Additionally, alveolar type II cells synthesize and secrete pulmonary surfactant (90–95% phospholipid) to reduce the surface tension of the alveolus [22]. Previous results have suggested the participation of phospholipid and sphingolipid metabolites in the inflammation of alveolar type II cells [48–51]. Therefore, the A549 alveolar type II cell line was used.

The levels of PC and sphingolipid metabolites were increased in BALF after $PM_{2.5}$ instillation *in vivo* but were decreased in A549 cells after BaP treatment *in vitro*. These findings may be due to the difference in stimulation that was used and involvement of other cells *in vivo*. The FFA levels were decreased after BaP treatment in A549 cells, a finding that seemed inconsistent with the increased PLA2 activity. This contradiction may be due to the increased catabolism of FFA in A549 cells. BaP and LPC upregulated the expression of cyclooxygenase-2 (COX-2) [52,53], which is responsible for the metabolism of ω–3 and ω–6 PUFA. In line with this, the proportion of PUFA was decreased after BaP treatment. ω–3 PUFA has been shown to have a markedly anti-inflammatory effect on different diseases by competing with the pro-inflammatory metabolism of the ω–6 PUFA cascade [54]. However, the ratio of ω–3/ω–6 PUFA was decreased after BaP treatment in these

cells, suggesting a weakened anti-inflammatory effect. In line with this, exogenous supplementation of ω–3 PUFA inhibited the inflammation induced by both $PM_{2.5}$ and BaP *in vivo* and *vitro* [55,56].

Activation of both cPLA2 and sPLA2 was found to mediate BaP-induced inflammation in A549 cells, a finding that was consistent with previous results [57]. The activation of cPLA2 was dependent on intracellular Ca^{2+} [24], and BaP increased intracellular Ca^{2+} in an aryl hydrocarbon receptor (AHR)-dependent manner [58], a finding that was also observed in this study. *Pla2g2a* was up regulated by BaP. PLA2g2a is often referred to as an "inflammatory sPLA2" and was markedly up regulated by pro-inflammatory stimuli and was correlated with the severity of inflammatory diseases [24]. However, the upregulation of *Pla2g2a* was not responsible for the increased generation of LPC because its upregulation occurred posterior to the increased PLA2 activity [59]. There is cross-talk between sPLA2 and cPLA2, and the upregulation of *Pla2g2a* may be due to the activation of cPLA2 and amplification of the inflammation induced by BaP. The expression of *Pla2g2a* has been proven to be inducible by the activation of cPLA2 in a peroxisome proliferator-activated receptor α-dependent manner [60].

This study indicated the participation of lipid metabolism in $PM_{2.5}$-induced pulmonary injury. BaP was further identified as one of the components of $PM_{2.5}$ and activated lipid metabolism in alveolar type II cells. BaP induced inflammation in A549 cells by activating phospholipid metabolism in a PLA2-dependent manner, suggesting that PLA2 may be a putative drug target for improving $PM_{2.5}$-induced pulmonary injury.

Grants

This work was supported by the National Natural Science Foundation of the P.R. China (31230035, 91439206 to X. Wang).

Author contributions

SY.Z. and D.S. designed and performed the experiments and analyzed the data. H.L. performed the HPLC-MS/MS and analyzed the data. J.F. designed the immunological experiments. D. S., Q. Z. and M. C. conducted the animal experiments. B.F. and X.S. prepared the $PM_{2.5}$ and took the scanning electron micrograph. X.W., W.H. and C.J. designed and supervised the research. SY.Z. and X.W. wrote the manuscript. All of the authors approved the final manuscript. The authors declare no competing financial interests. X.W and W.H. are the guarantors of this work and, as such, had full access to all of the data in the study and hold the responsibility for the integrity of the data and the accuracy of the analysis.

Acknowledgment

Rat pulmonary function was measured with the help of Prof. Bei He, Department of Respiration, Peking University Third Hospital, Peking University, Beijing, People's Republic of China. Song-Yang Zhang was supported in part by the Postdoctoral Fellowship of Peking-Tsinghua Center for Life Sciences.

Appendix A. Supporting information

Supplementary data associated with this article can be found in the online version at http://dx.doi.org/10.1016/j.redox.2017.07.001.

References

[1] H. Guo, Z.H. Ling, H.R. Cheng, I.J. Simpson, X.P. Lyu, X.M. Wang, M. Shao, H.X. Lu, G. Ayoko, Y.L. Zhang, S.M. Saunders, S.H. Lam, J.L. Wang, D.R. Blake, Tropospheric volatile organic compounds in China, Sci. Total Environ. 574 (2017) 1021–1043.
[2] Y.F. Xing, Y.H. Xu, M.H. Shi, Y.X. Lian, The impact of PM2.5 on the human respiratory system, J. Thorac. Dis. 8 (2016) E69–E74.
[3] H. Lin, T. Liu, J. Xiao, W. Zeng, X. Li, L. Guo, Y. Zhang, Y. Xu, J. Tao, H. Xian, K.M. Syberg, Z.M. Qian, W. Ma, Mortality burden of ambient fine particulate air pollution in six Chinese cities: results from the Pearl River Delta study, Environ. Int. 96 (2016) 91–97.
[4] Z. Bonyadi, M.H. Ehrampoush, M.T. Ghaneian, M. Mokhtari, A. Sadeghi, Cardiovascular, respiratory, and total mortality attributed to PM2.5 in Mashhad, Iran, Environ. Monit. Assess. 188 (2016) 570.
[5] J. Schwartz, D.W. Dockery, L.M. Neas, Is daily mortality associated specifically with fine particles? J. Air Waste Manag. Assoc. 46 (1996) 927–939.
[6] A.J. Badyda, J. Grellier, P. Dabrowiecki, Ambient PM2.5 exposure and mortality due to lung cancer and cardiopulmonary diseases in polish cities, Adv. Exp. Med. Biol. (2016).
[7] M. Simoni, S. Baldacci, S. Maio, S. Cerrai, G. Sarno, G. Viegi, Adverse effects of outdoor pollution in the elderly, J. Thorac. Dis. 7 (2015) 34–45.
[8] G.B. Hamra, N. Guha, A. Cohen, F. Laden, O. Raaschou-Nielsen, J.M. Samet, P. Vineis, F. Forastiere, P. Saldiva, T. Yorifuji, D. Loomis, Outdoor particulate matter exposure and lung cancer: a systematic review and meta-analysis, Environ. Health Perspect. 122 (2014) 906–911.
[9] W. Bernhard, Lung surfactant: Function and composition in the context of development and respiratory physiology. Annals of anatomy = Anatomischer Anzeiger: official organ of the Anatomische Gesellschaft, 2016.
[10] S.R. Shaikh, M.B. Fessler, K.M. Gowdy, Role for phospholipid acyl chains and cholesterol in pulmonary infections and inflammation, J. Leukoc. Biol. 100 (2016) 985–997.
[11] I. Sevastou, E. Kaffe, M.A. Mouratis, V. Aidinis, Lysoglycerophospholipids in chronic inflammatory disorders: the PLA(2)/LPC and ATX/LPA axes, Biochim. Biophys. Acta 1831 (2013) 42–60.
[12] X. Chu, X. Wei, S. Lu, P. He, Autotaxin-LPA receptor axis in the pathogenesis of lung diseases, Int. J. Clin. Exp. Med. 8 (2015) 17117–17122.
[13] Z. Leonenko, S. Gill, S. Baoukina, L. Monticelli, J. Doehner, L. Gunasekara, F. Felderer, M. Rodenstein, L.M. Eng, M. Amrein, An elevated level of cholesterol impairs self-assembly of pulmonary surfactant into a functional film, Biophys. J. 93 (2007) 674–683.
[14] M.B. Fessler, R.S. Summer, Surfactant lipids at the host-environment interface. Metabolic sensors, suppressors, and effectors of inflammatory lung disease, Am. J. Respir. Cell Mol. Biol. 54 (2016) 624–635.
[15] J. Lee, B. Yeganeh, L. Ermini, M. Post, Sphingolipids as cell fate regulators in lung development and disease, Apoptosis: Int. J. Program. Cell Death 20 (2015) 740–757.
[16] J. Tibboel, I. Reiss, J.C. de Jongste, M. Post, Sphingolipids in lung growth and repair, Chest 145 (2014) 120–128.
[17] W.L. Chen, C.Y. Lin, Y.H. Yan, K.T. Cheng, T.J. Cheng, Alterations in rat pulmonary phosphatidylcholines after chronic exposure to ambient fine particulate matter, Mol. Biosyst. 10 (2014) 3163–3169.
[18] Z. Yin, H.J. Xu, X.L. Yao, G. Liu, C.J. Nie, H. Wei, C. Li, M.L. Liang, Z.Y. Ming, X.J. Zhang, Ambient fine particles (PM2.5) attenuate collagen-induced platelet activation through interference of the PLCgamma2/Akt/GSK3beta signaling pathway, Environ. Toxicol. 32 (2017) 530–540.
[19] G. Matute-Bello, G. Downey, B.B. Moore, S.D. Groshong, M.A. Matthay, A.S. Slutsky, W.M. Kuebler, Acute lung injury in animals study G: an official American thoracic Society workshop report: featuresand measurements of experimental acute lung injury in animals, Am. J. Respir. Cell Mol. Biol. 44 (2011) 725–738.
[20] K. Tamakawa, Chapter 17 polycyclic aromatic hydrocarbons, Compr. Anal. Chem. 51 (2008) 599–651.
[21] R. Korhonen, A. Lahti, H. Kankaanranta, E. Moilanen, Nitric oxide production and signaling in inflammation, Curr. Drug Targets Inflamm. Allergy 4 (2005) 471–479.
[22] R.J. Mason, Biology of alveolar type II cells, Respirology 11 (2006) Suppl:S12–Suppl:S15.
[23] M. Murakami, Y. Taketomi, Y. Miki, H. Sato, T. Hirabayashi, K. Yamamoto, Recent progress in phospholipase A(2) research: from cells to animals to humans, Prog. Lipid Res. 50 (2011) 152–192.
[24] E.A. Dennis, J. Cao, Y.H. Hsu, V. Magrioti, G. Kokotos, Phospholipase A2 enzymes: physical structure, biological function, disease implication, chemical inhibition, and therapeutic intervention, Chem. Rev. 111 (2011) 6130–6185.
[25] D.R. Riva, C.B. Magalhaes, A.A. Lopes, T. Lancas, T. Mauad, O. Malm, S.S. Valenca, P.H. Saldiva, D.S. Faffe, W.A. Zin, Low dose of fine particulate matter (PM2.5) can induce acute oxidative stress, inflammation and pulmonary impairment in healthy mice, Inhal. Toxicol. 23 (2011) 257–267.
[26] R. Li, X. Kou, L. Xie, F. Cheng, H. Geng, Effects of ambient PM2.5 on pathological injury, inflammation, oxidative stress, metabolic enzyme activity, and expression of c-fos and c-jun in lungs of rats, Environ. Sci. Pollut. Res. Int. 22 (2015) 20167–20176.
[27] J. Grommes, O. Soehnlein, Contribution of neutrophils to acute lung injury, Mol. Med. 17 (2011) 293–307.
[28] M.P. Sierra-Vargas, A.M. Guzman-Grenfell, S. Blanco-Jimenez, J.D. Sepulveda-Sanchez, R.M. Bernabe-Cabanillas, B. Cardenas-Gonzalez, G. Ceballos, J.J. Hicks, Airborne particulate matter PM2.5 from Mexico City affects the generation of reactive oxygen species by blood neutrophils from asthmatics: an in vitro approach, J. Occup. Med. Toxicol. 4 (2009) 17.
[29] A. Montiel-Davalos, E. Alfaro-Moreno, R. Lopez-Marure, PM2.5 and PM10 induce the expression of adhesion molecules and the adhesion of monocytic cells to human umbilical vein endothelial cells, Inhal. Toxicol. 19 (Suppl 1) (2007) S91–S98.
[30] G. Wang, J. Zhao, R. Jiang, W. Song, Rat lung response to ozone and fine particulate matter (PM2.5) exposures, Environ. Toxicol. 30 (2015) 343–356.
[31] S.C. Jeong, Y. Cho, M.K. Song, E. Lee, J.C. Ryu, Epidermal growth factor receptor (EGFR)-MAPK-nuclear factor(NF)-kappaB-IL8: a possible mechanism of particulate

matter(PM) 2.5-induced lung toxicity, Environ. Toxicol. 32 (2017) 1628–1636.
[32] A.D. Luster, Chemokines–chemotactic cytokines that mediate inflammation, New Engl. J. Med. 338 (1998) 436–445.
[33] S. Goulaouic, L. Foucaud, A. Bennasroune, P. Laval-Gilly, J. Falla, Effect of polycyclic aromatic hydrocarbons and carbon black particles on pro-inflammatory cytokine secretion: impact of PAH coating onto particles, J. Immunotoxicol. 5 (2008) 337–345.
[34] V. Lecureur, E.L. Ferrec, M. N'Diaye, M.L. Vee, C. Gardyn, D. Gilot, O. Fardel, ERK-dependent induction of TNFalpha expression by the environmental contaminant benzo(a)pyrene in primary human macrophages, FEBS Lett. 579 (2005) 1904–1910.
[35] A.M. Knaapen, D.M. Curfs, D.M. Pachen, R.W. Gottschalk, M.P. de Winther, M.J. Daemen, F.J. Van Schooten, The environmental carcinogen benzo[a]pyrene induces expression of monocyte-chemoattractant protein-1 in vascular tissue: a possible role in atherogenesis, Mutat. Res. 621 (2007) 31–41.
[36] K. Sawyer, S. Mundandhara, A.J. Ghio, M.C. Madden, The effects of ambient particulate matter on human alveolar macrophage oxidative and inflammatory responses, J. Toxicol. Environ. Health Part A 73 (2010) 41–57.
[37] Q. Sun, A. Wang, X. Jin, A. Natanzon, D. Duquaine, R.D. Brook, J.G. Aguinaldo, Z.A. Fayad, V. Fuster, M. Lippmann, L.C. Chen, S. Rajagopalan, Long-term air pollution exposure and acceleration of atherosclerosis and vascular inflammation in an animal model, J. Am. Med. Assoc. 294 (2005) 3003–3010.
[38] Q. Sun, P. Yue, J.A. Deiuliis, C.N. Lumeng, T. Kampfrath, M.B. Mikolaj, Y. Cai, M.C. Ostrowski, B. Lu, S. Parthasarathy, R.D. Brook, S.D. Moffatt-Bruce, L.C. Chen, S. Rajagopalan, Ambient air pollution exaggerates adipose inflammation and insulin resistance in a mouse model of diet-induced obesity, Circulation 119 (2009) 538–546.
[39] G. Ramanathan, F. Yin, M. Speck, C.H. Tseng, J.R. Brook, F. Silverman, B. Urch, R.D. Brook, J.A. Araujo, Effects of urban fine particulate matter and ozone on HDL functionality, Part. Fibre Toxicol. 13 (2016) 26.
[40] T. Chen, G. Jia, Y. Wei, J. Li, Beijing ambient particle exposure accelerates atherosclerosis in ApoE knockout mice, Toxicol. Lett. 223 (2013) 146–153.
[41] Z. Xu, X. Xu, M. Zhong, I.P. Hotchkiss, R.P. Lewandowski, J.G. Wagner, L.A. Bramble, Y. Yang, A. Wang, J.R. Harkema, M. Lippmann, S. Rajagopalan, L.C. Chen, Q. Sun, Ambient particulate air pollution induces oxidative stress and alterations of mitochondria and gene expression in brown and white adipose tissues, Part. Fibre Toxicol. 8 (2011) 20.
[42] R. Mendez, Z. Zheng, Z. Fan, S. Rajagopalan, Q. Sun, K. Zhang, Exposure to fine airborne particulate matter induces macrophage infiltration, unfolded protein response, and lipid deposition in white adipose tissue, Am. J. Transl. Res. 5 (2013) 224–234.
[43] S. Breitner, A. Schneider, R.B. Devlin, C.K. Ward-Caviness, D. Diaz-Sanchez, L.M. Neas, W.E. Cascio, A. Peters, E.R. Hauser, S.H. Shah, W.E. Kraus, Associations among plasma metabolite levels and short-term exposure to PM2.5 and ozone in a cardiac catheterization cohort, Environ. Int. 97 (2016) 76–84.
[44] Y. Wei, Z. Wang, C.Y. Chang, T. Fan, L. Su, F. Chen, D.C. Christiani, Global metabolomic profiling reveals an association of metal fume exposure and plasma unsaturated fatty acids, PLoS One 8 (2013) e77413.
[45] B. Crestani, P. Cornillet, M. Dehoux, C. Rolland, M. Guenounou, M. Aubier, Alveolar type II epithelial cells produce interleukin-6 in vitro and in vivo. Regulation by alveolar macrophage secretory products, J. Clin. Investig. 94 (1994) 731–740.
[46] D.V. Pechkovsky, G. Zissel, M.W. Ziegenhagen, M. Einhaus, C. Taube, K.F. Rabe, H. Magnussen, T. Papadopoulos, M. Schlaak, J. Muller-Quernheim, Effect of proinflammatory cytokines on interleukin-8 mRNA expression and protein production by isolated human alveolar epithelial cells type II in primary culture, Eur. Cytokine Netw. 11 (2000) 618–625.
[47] J.N. Vanderbilt, E.M. Mager, L. Allen, T. Sawa, J. Wiener-Kronish, R. Gonzalez, L.G. Dobbs, CXC chemokines and their receptors are expressed in type II cells and upregulated following lung injury, Am. J. Respir. Cell Mol. Biol. 29 (2003) 661–668.
[48] R. Pawliczak, C. Logun, P. Madara, M. Lawrence, G. Woszczek, A. Ptasinska, M.L. Kowalski, T. Wu, J.H. Shelhamer, Cytosolic phospholipase A2 Group IValpha but not secreted phospholipase A2 Group IIA, V, or X induces interleukin-8 and cyclooxygenase-2 gene and protein expression through peroxisome proliferator-activated receptors gamma 1 and 2 in human lung cells, J. Biol. Chem. 279 (2004) 48550–48561.
[49] E. Pniewska, M. Sokolowska, I. Kuprys-Lipinska, M. Przybek, P. Kuna, R. Pawliczak, The step further to understand the role of cytosolic phospholipase A2 alpha and group X secretory phospholipase A2 in allergic inflammation: pilot study, BioMed. Res. Int. 2014 (2014) 670814.
[50] R. Newton, L. Hart, K.F. Chung, P.J. Barnes, Ceramide induction of COX-2 and PGE (2) in pulmonary A549 cells does not involve activation of NF-kappaB, Biochem. Biophys. Res. Commun. 277 (2000) 675–679.
[51] A. Billich, F. Bornancin, D. Mechtcheriakova, F. Natt, D. Huesken, T. Baumruker, Basal and induced sphingosine kinase 1 activity in A549 carcinoma cells: function in cell survival and IL-1beta and TNF-alpha induced production of inflammatory mediators, Cell. Signal. 17 (2005) 1203–1217.
[52] M.W. Weng, Y.M. Hsiao, C.J. Chen, J.P. Wang, W.C. Chen, J.L. Ko, Benzo[a]pyrene diol epoxide up-regulates COX-2 expression through NF-kappaB in rat astrocytes, Toxicol. Lett. 151 (2004) 345–355.
[53] V. Ruiperez, J. Casas, M.A. Balboa, J. Balsinde, Group V phospholipase A2-derived lysophosphatidylcholine mediates cyclooxygenase-2 induction in lipopolysaccharide-stimulated macrophages, J. Immunol. 179 (2007) 631–638.
[54] B. Lands, Omega-3 PUFAs lower the propensity for arachidonic acid cascade overreactions, BioMed. Res. Int. 2015 (2015) (285135).
[55] J. Gdula-Argasinska, J. Czepiel, J. Toton-Zuranska, P. Wolkow, T. Librowski, A. Czapkiewicz, W. Perucki, M. Wozniakiewicz, A. Wozniakiewicz, n-3 Fatty acids regulate the inflammatory-state related genes in the lung epithelial cells exposed to polycyclic aromatic hydrocarbons, Pharmacol. Rep.: PR 68 (2016) 319–328.
[56] I. Romieu, R. Garcia-Esteban, J. Sunyer, C. Rios, M. Alcaraz-Zubeldia, S.R. Velasco, F. Holguin, The effect of supplementation with omega-3 polyunsaturated fatty acids on markers of oxidative stress in elderly exposed to PM(2.5), Environ. Health Perspect. 116 (2008) 1237–1242.
[57] P.K. Tithof, M. Elgayyar, Y. Cho, W. Guan, A.B. Fisher, M. Peters-Golden, Polycyclic aromatic hydrocarbons present in cigarette smoke cause endothelial cell apoptosis by a phospholipase A2-dependent mechanism, FASEB J.: Off. Publ. Fed. Am. Soc. Exp. Biol. 16 (2002) 1463–1464.
[58] A. Mayati, E. Le Ferrec, D. Lagadic-Gossmann, O. Fardel, Aryl hydrocarbon receptor-independent up-regulation of intracellular calcium concentration by environmental polycyclic aromatic hydrocarbons in human endothelial HMEC-1 cells, Environ. Toxicol. 27 (2012) 556–562.
[59] T. Yano, D. Fujioka, Y. Saito, T. Kobayashi, T. Nakamura, J.E. Obata, K. Kawabata, K. Watanabe, Y. Watanabe, H. Mishina, S. Tamaru, K. Kugiyama, Group V secretory phospholipase A2 plays a pathogenic role in myocardial ischaemia-reperfusion injury, Cardiovasc. Res. 90 (2011) 335–343.
[60] S. Beck, G. Lambeau, K. Scholz-Pedretti, M.H. Gelb, M.J. Janssen, S.H. Edwards, D.C. Wilton, J. Pfeilschifter, M. Kaszkin, Potentiation of tumor necrosis factor alpha-induced secreted phospholipase A2 (sPLA2)-IIA expression in mesangial cells by an autocrine loop involving sPLA2 and peroxisome proliferator-activated receptor alpha activation, J. Biol. Chem. 278 (2003) 29799–29812.